Energy-averaged weak localization in chaotic microcavities

Mark W. Keller* and A. Mittal
Department of Applied Physics, Yale University, New Haven, Connecticut 06520-8284

J. W. Sleight
Department of Electrical Engineering, Yale University, New Haven, Connecticut 06520-8284

R. G. Wheeler and D. E. Prober
Department of Applied Physics and Department of Physics, Yale University, New Haven, Connecticut 06520-8284

R. N. Sacks†
United Technologies Research Center, East Hartford, Connecticut 06108

H. Shtrikmann
Weizmann Institute of Science, Braun Center for Submicron Research, Rehovot 76100, Israel
(Received 7 August 1995)

We have fabricated ballistic cavities from a two-dimensional GaAs electron gas in which the Fermi energy can be varied independent of cavity shape. For each cavity, we have measured the magnetoconductance $G(B)$ of many individual members of an ensemble, with each member labeled by its Fermi energy. We find that $G(B)$ of a single ensemble member does not always display the minimum at $B=0$ which is the signature of weak localization. By averaging over our ensemble, we have obtained the energy-averaged weak-localization effect for each cavity shape. The average result does display the expected minimum at $B=0$. We compare our results with recent analytical theories and numerical simulations of weak localization in cavities with chaotic classical scattering and find good quantitative agreement.

Two quantum interference effects due to multiply scattered electron waves, conductance fluctuations[1] and weak localization,[2] have been studied extensively in diffusive conductors, where electron scattering occurs on a length scale much smaller than the system size. Both effects have more recently been observed in ballistic cavities fabricated from the two-dimensional (2D) electron gas of a GaAs/Al_xGa_{1-x}As heterostructure, where large angle scattering is dominated by the edges of the cavities rather than by impurities. Ballistic quantum interference effects involving a magnetic field are governed by the distribution of enclosed areas in the classical analog of the cavity, according to a semiclassical analysis.[3] The area distribution is determined by the shape of the cavity and the size of the leads. For shapes in which classical particles scatter chaotically, the probability that a particle encloses an area A before escape is given by $P(A)\propto e^{-2\pi\alpha|A|}$.[3] The inverse area α determines the magnetic-field scale of the conductance fluctuations and the weak localization. For nonchaotic cavities the area distribution is not exponential and the semiclassical theory predicts the quantum interference will differ from that found in chaotic cavities. Experimental studies of conductance fluctuations as a function of magnetic field in chaotic cavities[4,5] agree well with the predictions of the semiclassical theory, and evidence for a difference between chaotic and nonchaotic shapes has been reported in one case.[4]

Here we focus on weak localization (WL) in ballistic cavities. We demonstrate that ballistic conductors do not ''self-average'' as do typical diffusive conductors used for the study of WL. This points out the need to average over an ensemble of cavities. We describe the fabrication of cavities in which the Fermi energy can be varied without changing the cavity shape. These cavities allow us to create many ensemble members and to construct the ensemble-averaged ballistic WL explicitly from the behavior of the individual members. Our results for three cavities with different shapes are in good quantitative agreement with theoretical predictions. We also discuss using the comparison with theory to estimate the amount of electron phase breaking in the cavities. We find that the contribution to WL from short paths interferes with a straightforward estimate of phase breaking.

The theoretical treatment of WL in diffusive conductors involves an average over an ensemble of conductors having

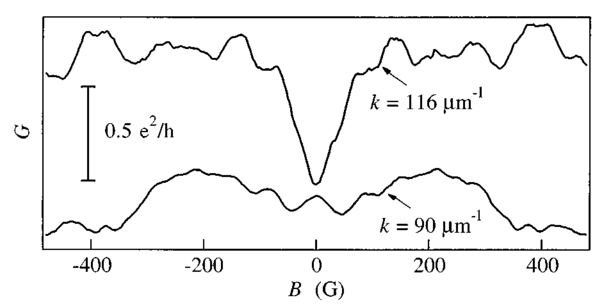

FIG. 1. $G(B)$ for the stomach at two values of the Fermi wave vector k. The upper curve shows the minimum at $B=0$ expected for the ensemble-average WL effect. The lower curve shows a maximum at $B=0$, demonstrating that a ballistic cavity does not self-average. The average WL can be found by averaging over many values of k, as described in the text.

different random configurations of impurities but the same macroscopic density of impurities. The theory predicts a decrease (relative to the classical value) in the ensemble-average conductance $\langle G\rangle$ of a phase-coherent conductor when time-reversal symmetry is present and spin-orbit scattering is negligible. Applying a magnetic field B destroys the WL and brings $\langle G\rangle$ back to its classical value. Thus, $\langle G(B)\rangle$ has a minimum at $B=0$. Experimental studies of WL in diffusive conductors typically involve samples many times larger than the phase coherence length. These samples effectively contain many members of an ensemble which are measured simultaneously (they are "self-averaging"). Thus, the measured $G(B)$ always has the minimum at $B=0$ expected for the ensemble average.

In contrast to the diffusive case, a ballistic cavity is normally smaller than the phase coherence length. It therefore represents a single member of an ensemble and does not necessarily behave as the ensemble average. This is demonstrated in Fig. 1, which shows a single ballistic cavity having a maximum in the measured G at $B=0$ for one value of the Fermi wave vector k, and a minimum for another value of k.[6] Previous experimental studies of WL in ballistic cavities have performed ensemble averages using temperature,[7] different realizations of residual disorder in an array of identical cavities,[8] or a small distortion of cavity shape.[9] Our experiments have the following characteristics: (1) Measurements were done at low temperature ($T\approx 100$ mK) where thermal averaging was negligible. (2) Different ensemble members were created by changing k using a gate voltage, so we could study individual members separately (as in Fig. 1). (3) The cavity size and shape did not change significantly over the range of k used for the ensemble average, as shown below. We designed our study with this combination of features in order to make the closest possible comparison to the theory of Ref. 3.

Recent theoretical work on WL in ballistic cavities has used three approaches: (1) Numerical calculation of the quantum $G(k)$ at different values of B for a particular cavity.[3] The WL is found by averaging over k at each value of B. This is precisely the way WL is measured in our experiments. (2) Analytical calculation of the energy-averaged WL using a semiclassical approximation.[3] (3) Calculation of the average WL for an ensemble of scattering matrices using a random matrix theory (RMT) approach.[10,11] The semiclassical and RMT analyses predict an inverted-Lorentzian form for the WL in chaotic cavities,

$$\langle \Delta G(B)\rangle \equiv \langle G(B)-G(0)\rangle = \Sigma\left[1-\frac{1}{1+(2B/\phi_0\alpha)^2}\right]. \tag{1}$$

The magnetic-field scale is the flux quantum, $\phi_0=h/e$, times the parameter of α from the classical area distribution. The value of α depends on the size and shape of the cavity, and on the size of the leads. The most recent RMT work of Baranger and Mello[10] predicts that the amplitude Σ varies with the number of modes in the leads, $N=kW/\pi$, and the number of effective phase-breaking modes, N_ϕ. They find

$$\Sigma=\frac{N}{2N+N_\phi}\frac{e^2}{h}, \tag{2}$$

which reduces to $\Sigma=(1/2)e^2/h$ at zero temperature ($N_\phi=0$) or $N\gg N_\phi$.

TABLE I. Cavity dimensions after subtracting a depletion width at each edge of 25 nm for the stadium and 85 nm for the stomach and polygon. Also given are the values of $\phi_0\alpha$ found from the power spectrum of the conductance fluctuations.

Cavity		Size (μm)	$\phi_0\alpha$ (G)
Stadium	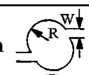	$R=0.28$ $W=0.15$	61 ± 5
Stomach		$L=1.4$ $W=0.21$	28 ± 2
Polygon	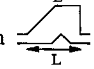	$L=1.3$ $W=0.21$	35 ± 2

In order to obtain ballistic cavities in which k could be varied independent of shape, we used two fabrication methods. The starting material in both cases was a GaAs/$Al_xGa_{1-x}As$ heterostructure with a 2D electron gas (2DEG) 90 to 100 nm below the surface. The low-energy ion exposure method,[12] used for the stadium, involved patterning a Ti/Au mask on the surface and exposing the sample to 200-eV Xe ions. The ions destroyed the conductivity in the unmasked regions. The metal mask then formed a self-aligned gate, and the electron density in the cavity could be increased or decreased by applying a positive or negative voltage between the gate and the 2DEG. The shallow wet etch method,[13] used for the stomach and polygon, involved patterning a poly-methylmethacrylate etch mask and etching 20 to 25 nm into the heterostructure using a solution of $NH_4OH/H_2O_2/H_2O$ (15:3:10 000). A Ti/Pd/Au gate of about 50 μm^2 area was then placed over the cavity and the insulating etched regions to vary the electron density.

The dimensions of each cavity are given in Table I and images are shown in Fig. 2. The bulk mean-free path of the 2DEG was 5.5 μm for the stadium and 19.5 μm for the stomach and polygon. We expect electron phase coherence to be limited by thermal dephasing, with a coherence length of 15 to 20 μm at the estimated electron temperature of 100 ± 50 mK. The electron density in the cavities n was found from oscillations in $G(B)$ that were periodic in $1/B$ for B larger than a few tesla, analogous to the Shubnikov–de Haas oscillations in a bulk 2DEG. We found that n changed linearly with gate voltage V_g, and k was computed using the 2D relation, $k=\sqrt{2\pi n}$. At $V_g=0$, k was 114 μm^{-1} for the stadium and 140 μm^{-1} for the stomach and polygon.

Our evidence that k can be changed without significantly affecting cavity size and shape is twofold. First, the field

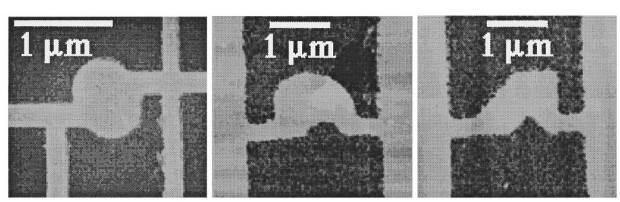

FIG. 2. Cavity images. The stadium image was obtained with a scanning electron microscope; the light areas are metal and the dark areas are the GaAs surface. The stomach and polygon images were obtained with a scanning force microscope; the light areas are unetched GaAs and the dark areas are etched to a depth of 23 nm.

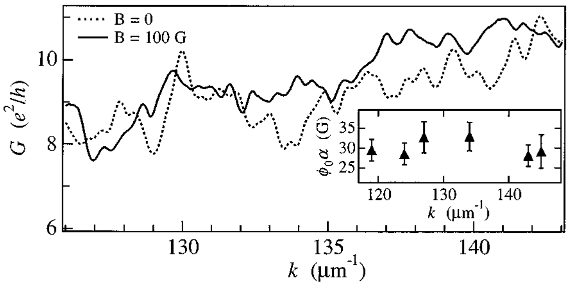

FIG. 3. Conductance fluctuations $G(k)$ for the stomach at $B=0$ and 100 G ($\approx 3.5\phi_0\alpha$). Inset: $\phi_0\alpha$ vs k for the stomach, which shows that changing k does not affect the typical area enclosed.

scale $\phi_0\alpha$ extracted from the power spectrum of the fluctuations in $G(B)$[4,5,16] was independent of k as shown for the stomach in the inset of Fig. 3. This indicates the typical area enclosed before escape from the cavity was independent of k. Second, studies of the ''last plateau'' in the Hall resistance of a cross junction[14] fabricated along with each cavity showed that the depletion width changed by 15%–20% over the range of k used for the WL studies. This corresponds to a change in W of about 15% and a change in L of about 2%. Using an approximate relation by Jensen,[15] these changes in cavity dimensions imply an expected change in $\phi_0\alpha$ of about 2%.

To construct the energy-averaged WL for each cavity, $G(k)$ was measured for many values of B between 0 and a few times $\phi_0\alpha$. Figure 3 shows $G(k)$ at $B=0$ and $B=100$ G for the stomach. The correlation range of the fluctuations in $G(k)$ is 0.56 μm^{-1},[16] so a change of k by this amount creates an independent member of the ensemble. The quantity $\Delta G(k,B) \equiv G(k,B) - G(k,0)$ is plotted for several values of B in Fig. 4. The range of k in this plot corresponds to 25 ensemble members, and the entire spectrum of behavior can be seen. At $k \approx 134$ μm^{-1}, ΔG increases as B increases, so $G(B)$ for this member of the ensemble looks like the upper curve in Fig. 1. At $k \approx 139.5$ μm^{-1}, ΔG is nearly 0 for all values of B, so $G(B)$ is flat near $B=0$. At $k \approx 128$ μm^{-1}, ΔG becomes negative as B increases, so $G(B)$ looks like the lower curve of Fig. 1. The ensemble-average WL, $\langle \Delta G(B) \rangle_k$, is found by simply taking the mean of each

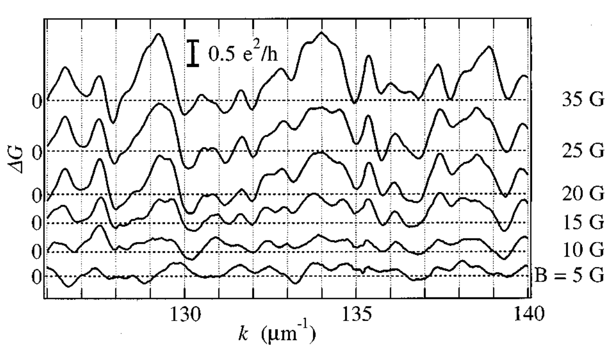

FIG. 4. $\Delta G(k,B) \equiv G(k,B) - G(k,0)$ for the stomach at several values of B between 0 and $\approx \phi_0\alpha$. The behavior of $G(B)$ for the 25 ensemble members shown in the figure ranges from a maximum at $B=0$ (e.g., $k \approx 128$ μm^{-1}) to a minimum at $B=0$ (e.g., $k \approx 134$ μm^{-1}).

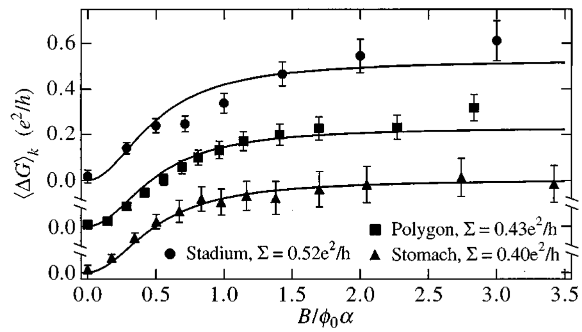

FIG. 5. The energy-averaged WL effect, $\langle \Delta G(B) \rangle_k$, for each of the three cavities. The energy ranges used to compute the averages correspond to $kW/\pi \approx [5.2,5.8]$ for the stadium, $kW/\pi \approx [7.6,9.1]$ for the stomach, and $kW/\pi \approx [8.0,9.9]$ for the polygon. The experimental points at $B=0$ represent the difference between two $G(k)$ traces before and after all the other traces and indicate the reproducibility of the data over long times (1–3 days). The solid lines are fits using Eq. (1) with the amplitude Σ as an adjustable parameter but with $\phi_0\alpha$ fixed at the value found from the fluctuations in $G(B)$. The legend shows the values of Σ found from the fits. The uncertainty in Σ is $\pm 0.04e^2/h$ for the stadium and $\pm 0.01e^2/h$ for the polygon and the stomach.

curve in Fig. 4, and the result for each cavity is shown in Fig. 5. The average change in G is positive, as expected, and the field scale over which the change occurs is $\phi_0\alpha$, also as expected.

Since we use the fluctuations in $G(B)$ to measure $\phi_0\alpha$ (values are given in Table I), we can fit Eq. (1) to $\langle \Delta G(B) \rangle_k$ using Σ as the only adjustable parameter. The result for each cavity is shown as a solid line in Fig. 5. The theory provides a good fit for the stomach and polygon, which show a clear saturation for $B \geqslant \phi_0\alpha$. The fit is not as good for the stadium, for which $\langle \Delta G(B) \rangle_k$ does not rise smoothly for $B \leqslant \phi_0\alpha$ and does not saturate as clearly at larger B. This behavior is not understood, but we note that some cavities studied numerically did not show a clear saturation.[3] The good agreement shown in Fig. 5 indicates that the same $\phi_0\alpha$ determines both the WL and the fluctuations, as predicted by the theories of the two effects.[3]

By comparing the value of Σ from the fits with Eq. (2), we can infer the effective number of phase-breaking channels N_ϕ. We find $N_\phi = 4.7 \pm 1.2$ for the stomach and $N_\phi = 2.9 \pm 1.0$ for the polygon. The uncertainty in these values comes from the uncertainty in Σ and from the range of $N = kW/\pi$ used in the energy average. N_ϕ is two to four times smaller than N, indicating that most electrons escape through the leads before losing phase coherence. For the stadium, Eq. (2) gives $N_\phi \approx 0$, but since Eq. (1) does not provide a good fit to $\langle \Delta G(B) \rangle_k$ for this cavity, we do not consider this a reliable measure of N_ϕ.

WL in the stomach and polygon shapes has been computed numerically,[3] and we compare the results with our data in Fig. 6. This is a direct comparison with no fitting involved. For the stomach, the agreement is very good. In fact, such good agreement raises a question about the reliability of using the WL amplitude Σ to determine N_ϕ as described above. Since numerical simulations done for $T=0$ can give Σ smaller than $0.5e^2/h$, there must be factors other than phase breaking that can reduce Σ. Thus, a measured Σ of less than

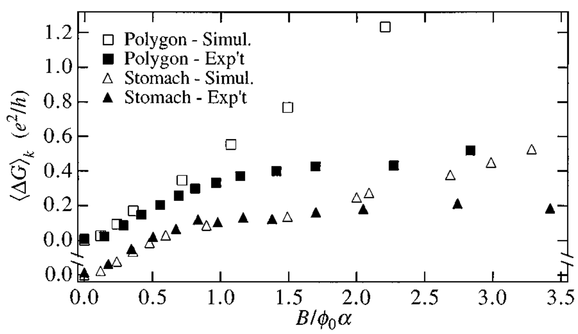

FIG. 6. Comparison of the WL for the stomach and polygon with numerical simulations for the same shapes.

$0.5e^2/h$ in a particular cavity does not necessarily imply that N_ϕ is greater than zero. The reduced amplitude in the simulations is believed to arise from the existence of short paths, such as those which bounce off the stopper that blocks direct transmission and back into the same lead or bounce once off the top of the cavity and into the opposite lead.[17] Such paths are explicitly omitted in the RMT approach which gives $\Sigma = 0.5e^2/h$ at $T=0$. Short paths are present in the experimental cavities, and a quantitative understanding of their effect on the WL is required in order to determine N_ϕ from the WL amplitude. This point has not been made previously when experimental values of Σ have been used to infer N_ϕ. In the case of the stomach, short paths reduce the amplitude of the simulation to $\Sigma \approx 0.4e^2/h$, the same as the experimental value. This could be interpreted as an indication that $N_\phi \approx 0$ (i.e., $N_\phi \ll N$). However, since the short paths are sensitive to details of the cavity shape, an unambiguous determination of N_ϕ may require knowledge of the experimental shape at a level of detail that is not possible using current nanofabrication techniques.[18]

For the polygon, the numerical result for $\langle \Delta G(B) \rangle_k$ is linear from near $B=0$ to well beyond $B=\phi_0\alpha$. This behavior is characteristic of nonchaotic scattering in the classical analog of the cavity, as is found for the ideal polygon shape[3] and for a circular cavity in a recent experiment.[8] We attribute the lack of agreement between the numerical and experimental results for the polygon to residual disorder which causes deviations from the ideal shape that are sufficient to make the classical scattering chaotic. This is consistent with the fact that the power spectrum of fluctuations in $G(B)$ for the polygon can be fit well with the form for chaotic scattering.[16]

In summary, we have measured the weak-localization effect in ballistic cavities and observed behavior which clearly differs from that of diffusive conductors. By using cavities in which the Fermi energy can be changed without affecting the cavity shape, we have measured the magnetoconductance of many individual members of an ensemble. The weak-localization effect found by averaging over this ensemble is generally in good agreement with analytical theories and numerical simulations for cavities with chaotic classical scattering.

This research was supported by Contract No. DMR-9112752. Photolithography masks were made at the Cornell National Nanofabrication Facility and sample fabrication was done at the Yale Center for Microelectronic Materials and Structures. We thank Doug Stone, Harold Baranger, and Charlie Marcus for many helpful conversations, and Mark Amman for providing scanning force microscope images.

*Present address: National Institute of Standards and Technology, Division 814.03, Boulder, CO 80303-3328. Electronic address: mark.keller@boulder.nist.gov.

†Present address: Department of Electrical Engineering, Ohio State University, Columbus, OH 43210.

[1] P. A. Lee, A. D. Stone, and H. Fukuyama, Phys. Rev. B **35**, 1039 (1987).

[2] G. Bergmann, Phys. Rep. **107**, 1 (1984).

[3] R. A. Jalabert, H. U. Baranger, and A. D. Stone, Phys. Rev. Lett. **65**, 2442 (1990); H. U. Baranger, R. A. Jalabert, and A. D. Stone, Phys. Rev. Lett. **70**, 3876 (1993); Chaos **3**, 665 (1993).

[4] C. M. Marcus, A. J. Rimberg, R. M. Westervelt, P. F. Hopkins, and A. C. Gossard, Phys. Rev. Lett. **69**, 506 (1992).

[5] M. W. Keller, O. Millo, A. Mittal, D. E. Prober, and R. N. Sacks, Surf. Sci. **305**, 501 (1994).

[6] According to the ergodic hypothesis described in Ref. 1, changing k and changing the impurity configuration are equivalent ways of creating different ensemble members.

[7] M. J. Berry, J. A. Katine, C. M. Marcus, R. M. Westervest, and A. C. Gossard, Surf. Sci. **305**, 495 (1994); M. J. Berry, J. H. Baskey, R. M. Westervest, and A. C. Gossard, Phys. Rev. B **50**, 8857 (1994).

[8] A. M. Chang, H. U. Baranger, L. N. Pfieffer, and K. W. West, Phys. Rev. Lett. **73**, 2111 (1994).

[9] I. H. Chan, R. M. Clarke, C. M. Marcus, K. Campman, and A. C. Gossard, Phys. Rev. Lett. **74**, 3876 (1995).

[10] H. U. Baranger and P. A. Mello, Phys. Rev. Lett. **73**, 142 (1994); Phys. Rev. B **51**, 4703 (1995).

[11] Z. Pluhar, H. A. Weidenmüller, J. A. Zuk, and C. H. Lewenkopf, Phys. Rev. Lett. **73**, 2115 (1994).

[12] A. Scherer and M. L. Roukes, Appl. Phys. Lett. **55**, 377 (1989); F. Li, G. F. Spencer, T. Wang, C. C. Andrews, and W. P. Kirk, J. Vac. Sci. Technol. B **11**, 2592 (1993).

[13] K. Y. Lee, D. P. Kern, K. Ismail, and S. Washburn, J. Vac. Sci. Technol. B **9**, 2834 (1991).

[14] C. W. J. Beenakker and H. van Houten, in *Electronic Properties of Multilayers and Low-Dimensional Semiconductor Structures*, edited by J. M. Chamberlain, L. Eaves, and J. C. Portal (Plenum, New York, 1990).

[15] R. V. Jensen, CHAOS **1**, 101 (1991).

[16] M. W. Keller, Ph.D. thesis, Yale University, 1995, available from University Microfilms, Ann Arbor, MI; M. W. Keller *et al.* (unpublished).

[17] H. U. Baranger (private communication).

[18] We note that the existence of short paths does not affect the determination of $\phi_0\alpha$ from the fluctuations in $G(B)$ because the power spectrum fitting is done only for the longer paths. In this sense, α is a more "universal" parameter of chaotic cavities than Σ.